

Chapter 5

Diethyl disulfo-ammonium chlorometallates: A novel and reusable heterogeneous acidic catalyst for the multicomponent synthesis of 14-aryl-7-(N-phenyl)-14*H*-dibenzo[*a,j*]acridine derivatives

5.1. Introduction

Ionic liquids incorporated with metal chlorides commonly known as chlorometallate ionic liquids (ILs). Chloroaluminates (III) were the first example of such type of Lewis acidic ionic liquids that received growing attention in the field of catalysis [1-2]. However, their applications were limited due to their hygroscopic nature. The anionic composition determines the properties of chlorometallates which again depends on the types of metal chloride and the ratios of metal chloride to parent organic chloride [3-5]. The various developments of such ionic salts over the last two decade have recognized these chlorometallates/halometallates as functional materials with unique and useful properties including photo physical, magnetic, catalytic and semiconductors etc. [6-8]. Some of them can be developed as air/water stable-ionic salts by varying the type of cationic and anionic compositions and also the concentration of metal halides that directly relates to characteristic and individual properties. Gogoi *et al* developed $-\text{SO}_3\text{H}$ functionalized 1-methyl-imidazolium based chlorometallates of Fe(III) and Zn(II) as Brønsted-Lewis acidic heterogeneous catalyst for the preparation of bis(indolyl)methane derivatives under mild condition [9]. Saikia *et al* also prepared 1, 3-disulfoimidazolium based chlorometallates of Fe(III) and Zn(II) as bi-functionalized acidic material for the Mannich-type reaction at ambient temperature in solution [8]. The above chlorometallates bearing $-\text{SO}_3\text{H}$ group provided higher thermal and water stabilities in presence of metal chlorides [8]. Herein, we aimed to synthesize bi-functionalized diethyl disulfo ammonium chlorometallates ($[(\text{Et})_2\text{N}(\text{SO}_3\text{H})_2]_n[\text{X}]$), where $n = 1$ or 2 for $\text{X} = \text{FeCl}_4^-$ (**IL-14**) and $\text{Zn}_2\text{Cl}_6^{2-}$ (**IL-15**) from the reaction of diethyldisulfoammonium chloride ionic liquid $[(\text{Et})_2\text{N}(\text{SO}_3\text{H})_2][\text{Cl}]$ (**IL-13**) with respective transition metal chloride (FeCl_3 and ZnCl_2) at 80°C under solvent-free condition (**Scheme-5.1**). The ammonium based three acidic ionic liquid systems were characterized by various analytical techniques and then subjected for UV/Vis acidity study and thermogravimetric analysis.

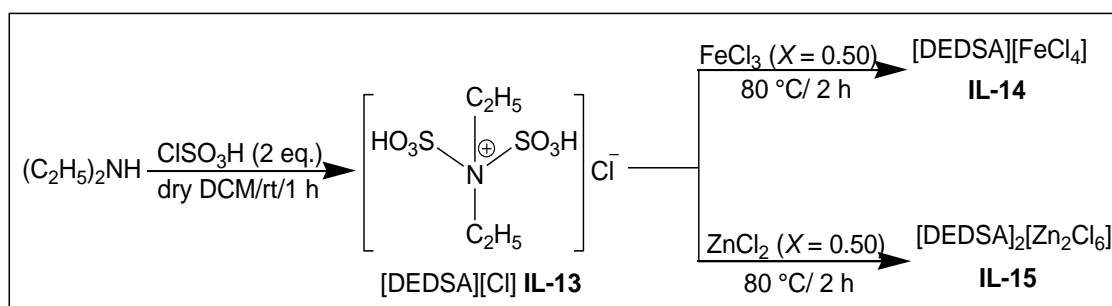
The catalytic performances of these chlorometallates were examined for the three-component synthesis of 14-aryl-7-(N-phenyl)-14*H*-dibenzo[*a,j*]acridine derivatives (**1**) from the reaction of equimolar mixture of 2-naphthol, N-phenyl-2-naphthylamine and aromatic aldehyde under solvent-free method at 100°C . The benzoacridine derivatives have wide range of pharmacological activities and uses in material science that already discussed in the **Chapter 1 (Section 1.1c)**. The literature review revealed lack of efficient

methodologies for the synthesis of different types of dibenzoacridine derivatives. Dutta *et al* in 2003 prepared few N-alkyl- derivatives of acridine, benzo[c]acridine and dibenzo[c,h]acridine in dry THF at 0 °C through treatment of these basic units with phenyllithium-TMEDA and then quenching the reaction mixture in D₂O or alkyl halide [10]. Later on, in 2006 Benniston *et al* isolated 14-phenyl-7-N-phenyl-dibenzo[a,j]acridine as unoptimized reaction intermediate with 22 % yield by refluxing the equimolar mixture of 2-naphthol, N-phenyl-2-naphthylamine and benzaldehyde in glacial acetic acid [11]. The synthesis of 14-aryl-7, 14- dihydrodibenzo[a,j]acridine derivatives was exploited by Tu *et al* via one-pot reaction of 2-naphthylamine and various aromatic aldehyde under MWI in presence of thiosalicylic acid catalyst within short time [12]. The same synthesis was also carried out by Osyanin *et al* (2014) from the reaction of Betti base with 2-naphthylamine in acetic acid for 6 hour in argon atmosphere to get 20-50 % of 14-aryl-7,14- dihydrodibenzo[a,j]acridine [13].

5.2. Results and Discussion

5.2.1. Preparation and characterization of diethyl-disulfoammonium chlorometallates

Two bifunctionalized Brønsted-Lewis acidic diethyl-disulfoammonium chlorometallate ionic liquids [DEDSA]_n[X], where n = 1 and 2 for X = FeCl₄⁻ (**IL-14**) and Zn₂Cl₆²⁻ (**IL-15**) respectively were prepared by treating ionic liquid [(Et)₂N(SO₃H)₂][Cl] (**IL-13**) with corresponding transition metal chlorides (FeCl₃ and ZnCl₂) at 80 °C in neat condition for 2 hour (**Scheme- 5.1**).



Scheme-5.1: Preparation of diethyl disulfo-ammonium chlorometallates

5.2.1.1. Spectral analysis

The infrared spectra of three ionic liquid systems displayed characteristic bands of $-\text{SO}_3\text{H}$ group in **Fig.5.1**. For example, the strong symmetric and anti-symmetric stretching vibrations of S-O bond observed at $1147\text{--}1166\text{ cm}^{-1}$ and $1044\text{--}1052\text{ cm}^{-1}$ respectively. The strong stretching vibration at $869\text{--}879\text{ cm}^{-1}$ can be attributed for N-S bond which confirmed the attachments of $-\text{SO}_3\text{H}$ groups with the ammonium nitrogen. Two small peaks around $1362\text{--}1385\text{ cm}^{-1}$ and $1408\text{--}1427\text{ cm}^{-1}$ can be assigned for C-H bending and rocking vibration of methyl groups. The $-\text{OH}$ broad band observed at $3380\text{--}3420\text{ cm}^{-1}$.

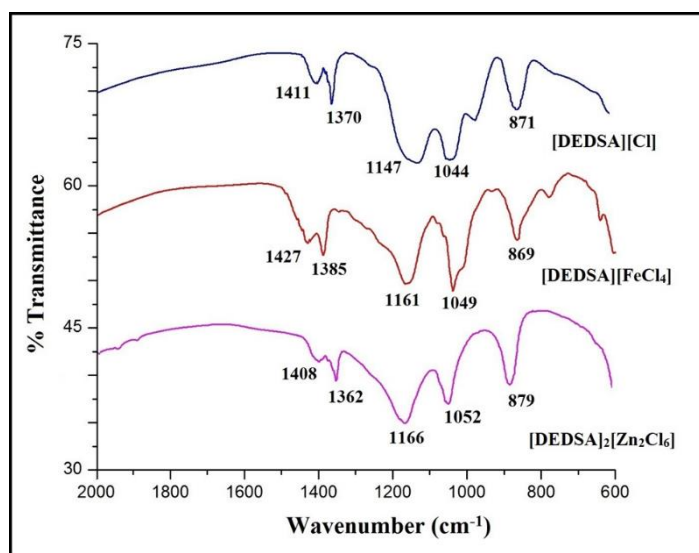


Fig.5.1: FT-IR spectra of disulfonic ammonium ionic liquids system

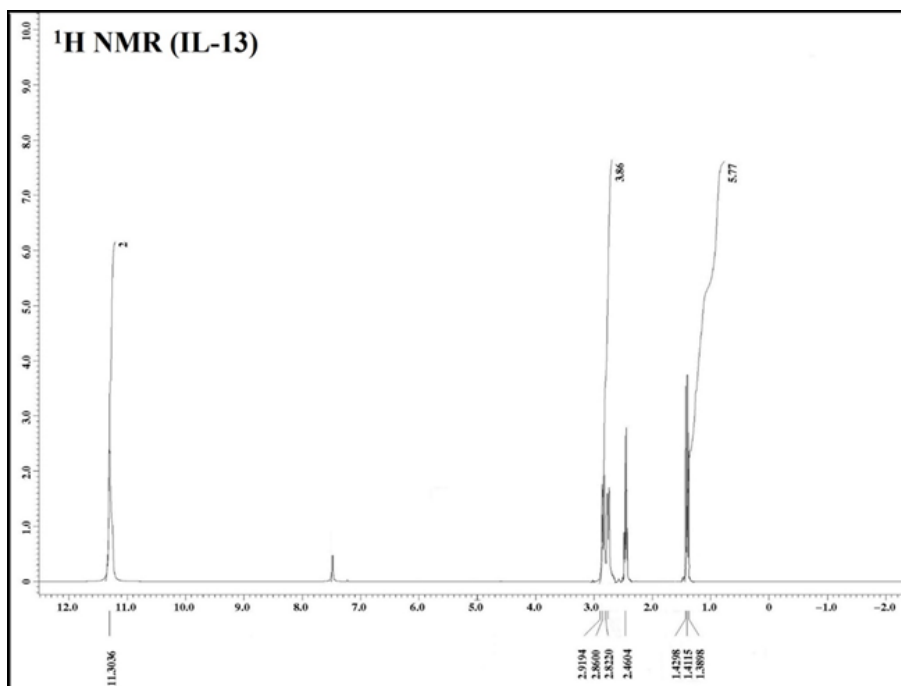


Fig.5.2a: ^1H NMR spectra of [DEDSA][Cl]

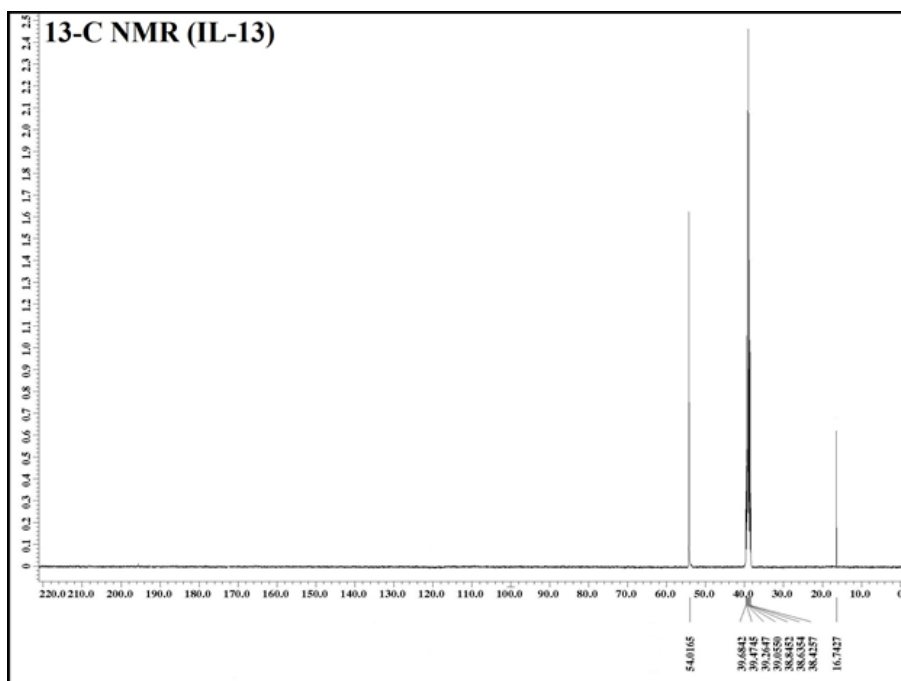


Fig.5.2b: ^{13}C NMR spectra of $[\text{DEDSA}][\text{Cl}]$

The ^1H NMR spectra of $[\text{DEDSA}][\text{Cl}]$ (**IL-13**) in **Fig.5.2a** shows one two proton singlet at $\delta = 11.3$ ppm for two $-\text{SO}_3\text{H}$ groups. The same spectra also indicated the presence of two ethyl groups with a triplet at 1.41 ppm for six $-\text{Me}$ proton and a multiplet around 2.82-2.92 ppm for four $-\text{CH}_2-$ proton. Similarly, the ^{13}C NMR spectrum of this IL represented $-\text{CH}_3$ carbon at 16.7 ppm and $-\text{CH}_2-$ carbon at 54 ppm in the **Fig.5.2b**. The lower solubility of two chlorometallates in $\text{DMSO}-d_6$ restricted their NMR study.

5.2.1.2. Study of surface morphology

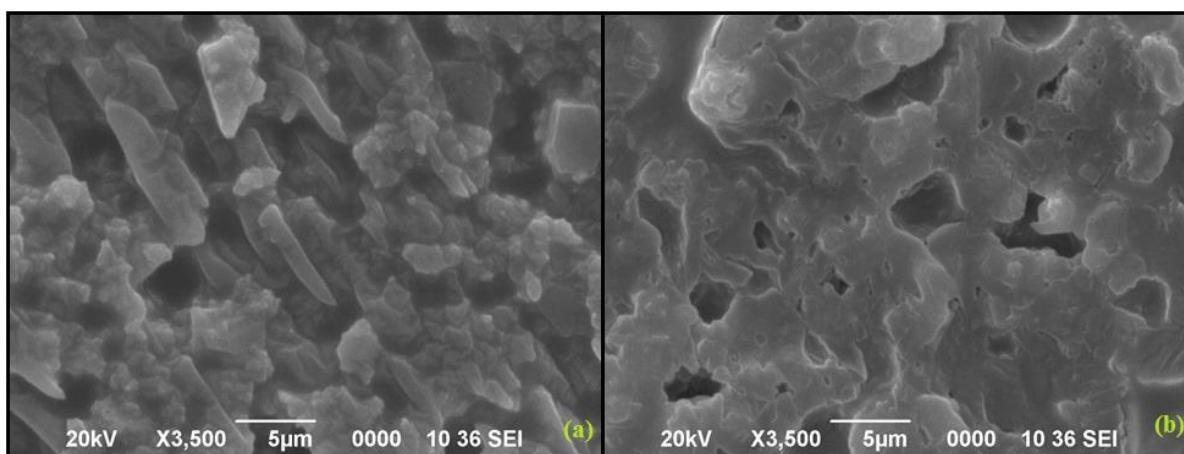


Fig.5.3: SEM images of (a) $[\text{DEDSA}][\text{FeCl}_4]$ (b) $[\text{DEDSA}]_2[\text{Zn}_2\text{Cl}_6]$

Scanning electron microscopy (SEM) images identify unique types of surface morphology for the two chlorometallates in **Fig.5.3**. The image of Fe salt has distribution of some rod-like structure with non-uniform aggregation of small or medium size particles. The surface of Zn salt appears as highly viscous material distributed as plain surfaces with various size holes without any aggregations.

5.2.1.3. EDX analysis

The energy dispersion X-ray (EDX) analysis confirmed the presence of corresponding constituent elements of the chlorometallates on their surfaces as shown in **Fig.5.4**.

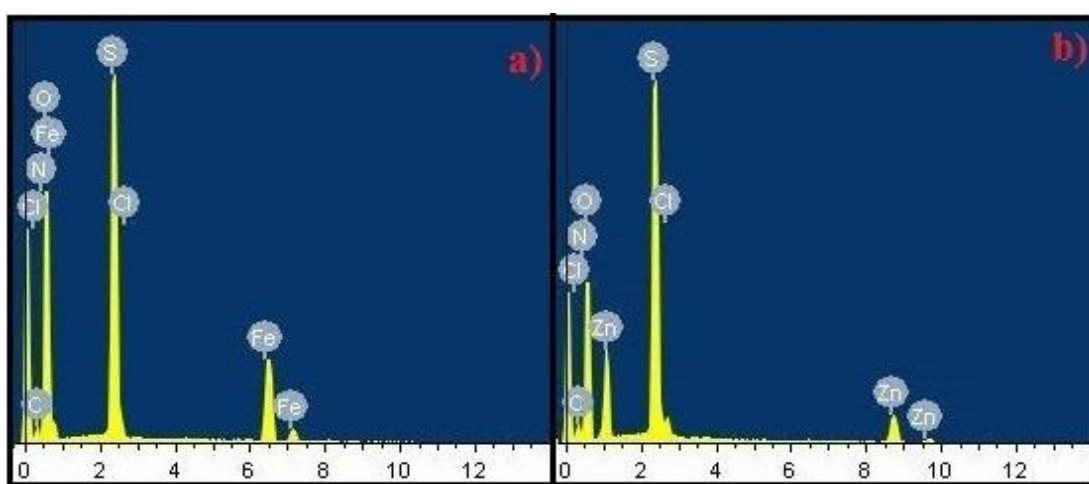


Fig.5.4: EDX analysis of (a) [DEDSA][FeCl₄] (b) [DEDSA]₂[Zn₂Cl₆]

5.2.1.4. Powder X-ray diffraction analysis

Powder X-ray diffraction analysis (PXRD) exhibits several peaks with sharp intensity for the chlorometallate ILs viz. [DEDSA][FeCl₄] and [DEDSA]₂[Zn₂Cl₆] as shown in **Fig.5.5**. The peaks at $2\theta = 15.1^\circ, 33.0^\circ, 33.5^\circ$ and 42.5° for Fe salt were matched well for the planes (0, 0,12), (1,1,-12), (0,0,26) and (0,0,-24) of JCPDS-770999. Likewise, for Zn salt, the observed 2θ values at $16.2^\circ, 25.3^\circ, 29.2^\circ$ and 48.1° can be assigned for the planes (0,0,2), (1,0,1), (1,0,2) and (1,1,4) from the literature data (JCPDS-704517). All these data confirm the existence of metal chlorides in the ionic solid chlorometallates.

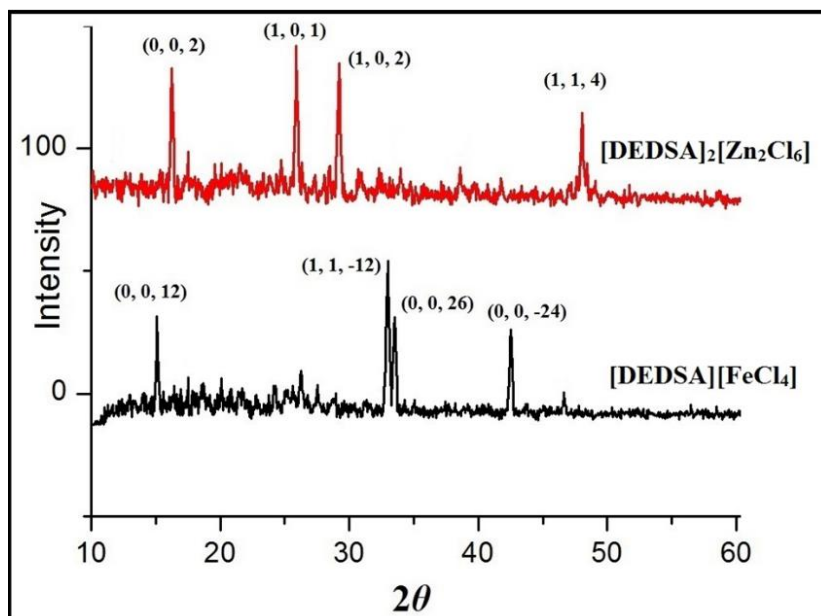


Fig.5.5: Powder XRD pattern of (a) [DEDSA][FeCl₄] (b) [DEDSA]₂[Zn₂Cl₆]

5.2.1.5. Raman analysis

In the Raman spectrum (**Fig.5.6**) a sharp peak at 332 cm⁻¹ for [DEDSA][FeCl₄] confirms the presence of FeCl₄⁻ in the chlorometallate [14]. Similarly the composition of Zn salt exhibited characteristic peaks of dimeric Zn₂Cl₆²⁻ anion at 257 cm⁻¹ and 315 cm⁻¹ in agreement with the literature values [15]

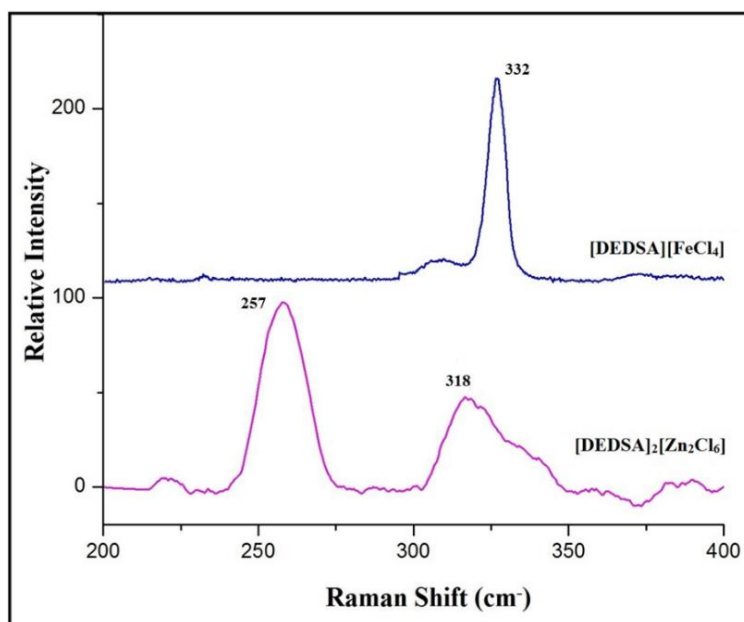


Fig.5.6: Raman spectra of (a) [DEDSA][FeCl₄] (b) [DEDSA]₂[Zn₂Cl₆]

5.2.1.6. Hammett plot for acidity study

The Brønsted acidity of two chlorometallates and parent IL was determined from the Hammett plot (**Fig.5.7**) via UV/Vis spectrophotometer using 4-nitroaniline as basic indicator according to the standard procedure discussed in the **Chapter-2**. From this experiment the Brønsted acidity of the ILs in decreasing order are $[\text{DEDSA}][\text{FeCl}_4] > [\text{DEDSA}]_2[\text{Zn}_2\text{Cl}_6] > [\text{DEDSA}][\text{Cl}]$ which is also supported by H^o value calculated (**Table-5.1**) for these ILs.

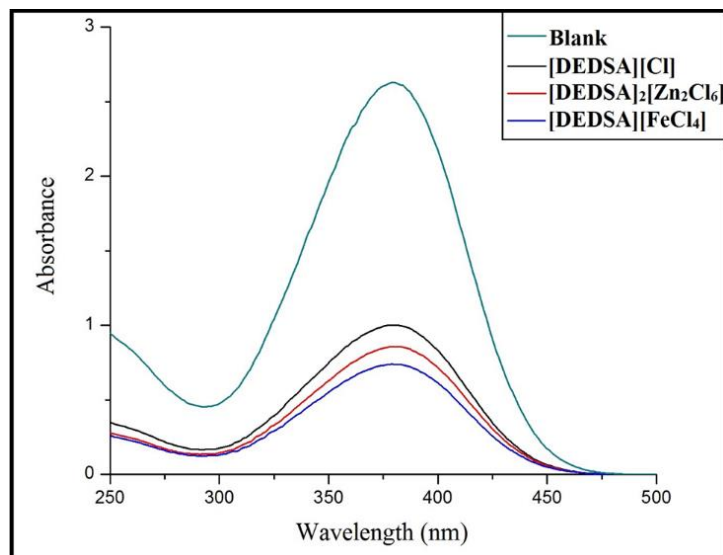


Fig.5.7: Hammett plot of three diethyldisulfoammonium based ionic salts

Table-5.1: Values of Hammett function for the three ILs

Entry	IL	λ_{max}	[I]%	[IH]%	H^o
1	Blank	2.63	100.0	0	-
2	$[\text{DEDSA}]\text{Cl}$	1.00	38.02	61.98	0.78
3	$[\text{DEDSA}]_2[\text{Zn}_2\text{Cl}_6]$	0.86	32.70	67.30	0.68
4	$[\text{DEDSA}][\text{FeCl}_4]$	0.74	28.14	71.86	0.58

5.2.1.7. Thermogravimetric analysis (TGA)

Thermogravimetric analysis was used to determine the thermal stability of the chlorometallates as well as the parent IL as shown in **Fig.5.8**. The TGA curve of $[\text{DEDSA}][\text{Cl}]$ ionic liquid showed approximately 20 % weight loss for elimination of adsorbed moisture at 100 °C which was reduced to 5-8 % for the two chlorometallates and

thus represent the less hygroscopic nature of Fe and Zn containing ionic salts. For Zn salt, around 20 % weight loss was observed in the temperature range of 140-300 °C which can be attributed for elimination of $-\text{SO}_3\text{H}$ groups. Similarly the 2nd decomposition of Fe salt started around 300 °C which is higher than both $[\text{DEDSA}][\text{Cl}]$ and $[\text{DEDSA}]_2[\text{Zn}_2\text{Cl}_6]$.

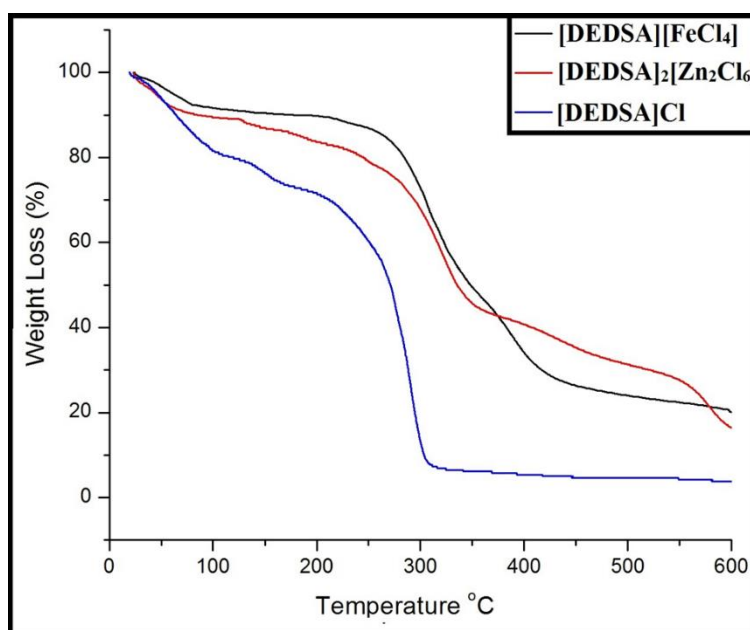


Fig.5.8: TGA curves of three diethyldisulfoammonium based ionic salts

5.2.1.8. Electronic spectroscopy

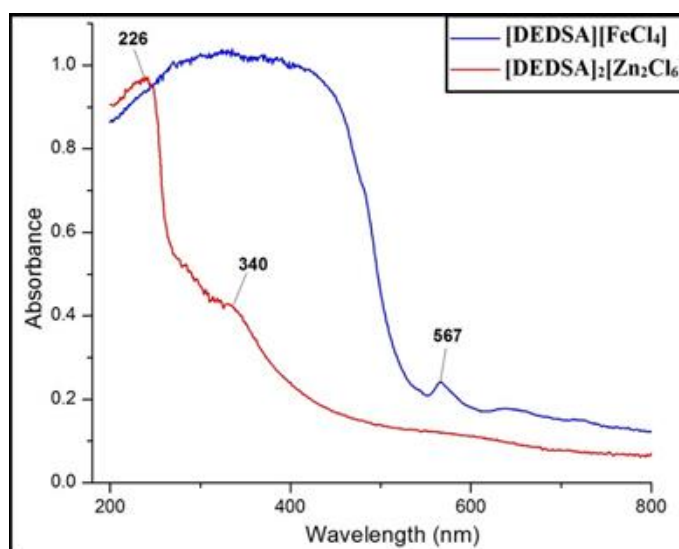


Fig.5.9: Electronic spectra of chlorometallates

Solid-UV analysis was employed in support to determine the composition of anionic species of the two chlorometallates, **IL-14** and **IL-15** which is shown in **Fig.5.9**. It was

observed that for the Fe salt the transition for ligand to metal charge transfer in the range of 270-380 nm is merged with a broad peak around 250-450 nm. It also displayed another weak d-d transition at 567 nm for FeCl_4^- anion [16-17]. Similarly the two absorption peaks around 226 nm and 340 nm for the Zn salt can be assigned as inter ligand charge transfer transitions of two tetrahedral ZnCl_4^- which are present in $\text{Zn}_2\text{Cl}_6^{2-}$ anion via two bridging Cl ligand [18]. The determination of anionic component of the chlorometallate ILs through solid-UV analysis provides well support to the Raman study.

5.2.1.9. Elemental analysis

The quantity of C, H and N present in the [DEDSA][Cl] and two chlorometallate salts was determined in CHN elemental analyzer after heating the samples in vacuum oven at 80 °C for one hour which are included in the spectral data. The amount of metal contents in the two diethyl disulfoammonium transition metal chlorides were measured by performing Inductively Coupled Plasma (ICP) elemental analysis with 10 ppm solution of each solid ionic salt in aqua-regia. The results obtained in **Table-5.2** were very close to the calculated value which confirms the actual combination of metal chlorides with the [DEDSA][Cl] for the formation of ionic salts **IL-14** and **IL-15**.

Table-5.2: ICP analyses for metal content of the disulfoammonium chlorometallates

Entry	Sample	Mol. weight (gm/mol)	Atom. weight of metal (gm/mol)	Amt. of the metal (mg/liter)		
				Exp.	Cal.	Spent catalyst (after 6 th cycle)
1	[DEDSA][FeCl ₄]	403.88	55.85	1.38	1.43	1.01
2	[DEDSA] ₂ [Zn ₂ Cl ₆]	755.94	130.76	1.73	1.76	1.17

5.2.1.10. Leaching test

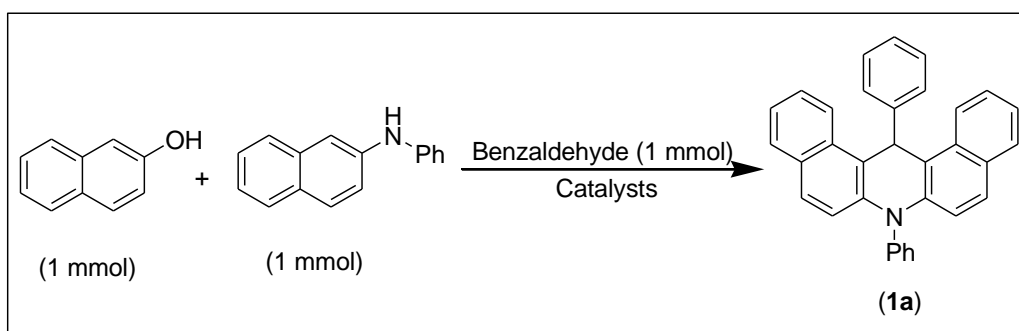
Leaching test of [DEDSA][FeCl₄] and [DEDSA]₂[Zn₂Cl₆] was carried out by stirring 50 mg of each in four different solvents (5mL) separately viz EtOH, CH₃CN, CH₂Cl₂ and H₂O for 3 h at room temperature. Except water, the pH of three filtrates was found as neutral values. The pH of water solution observed at 5 and expressed slight solubility or leaching of acidic component in presence of the water as solvent.

5.2.2. Catalytic activity study

5.2.2.1. Optimization of reaction condition

The catalytic activity of [DEDSA][FeCl₄] and [DEDSA]₂[Zn₂Cl₆] chlorometallates was explored for the three-component synthesis of 14-aryl-7-N-phenyl-14*H*-dibenzo[*a,j*]acridine derivatives (**1**) according to the reaction scheme included in **Table-5.3** and **Table-5.4** starting from a mixture of 2-naphthol, aromatic aldehydes and *N*-2-naphthylamine in solvent-free condition.

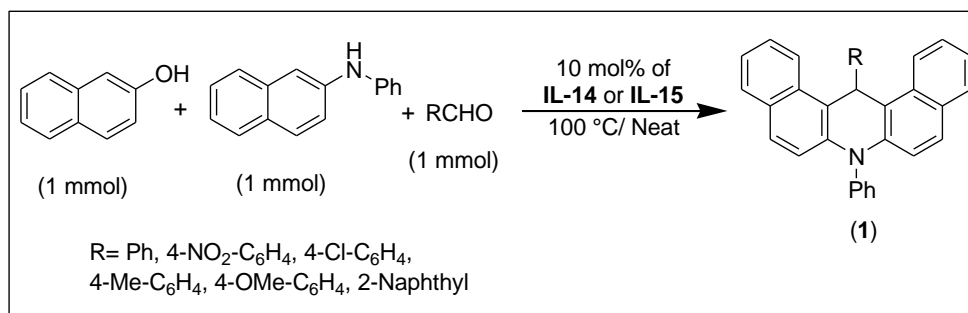
Table--5.3: Optimization of the reaction condition



Entry	Catalyst	Cat. (mol%)	Temp (°C)	Time (min)	% of yield ^a (1a)
1	[DEDSA][FeCl ₄]	15	110	45	84
2	[DEDSA][FeCl ₄]	15	100	45	84
3	[DEDSA][FeCl ₄]	15	90	50	81
4	[DEDSA][FeCl ₄]	10	100	45	84
5	[DEDSA][FeCl ₄]	8	100	55	77
6	[DEDSA] ₂ [Zn ₂ Cl ₆]	15	110	50	81
7	[DEDSA] ₂ [Zn ₂ Cl ₆]	15	100	50	81
8	[DEDSA] ₂ [Zn ₂ Cl ₆]	15	90	1 h	75
9	[DEDSA] ₂ [Zn ₂ Cl ₆]	10	100	50	81
10	[DEDSA] ₂ [Zn ₂ Cl ₆]	8	100	65	70

^a Isolated yields;

Table-5.4: Synthesis of 14-aryl-7-N-phenyl-14*H*-dibenzo[*a,j*]acridines (**1**) using **IL-14** and **IL-15** as catalysts



Entr y	R	[DEDSA][FeCl ₄]		[DEDSA] ₂ [Zn ₂ Cl ₆]	
		Time	% of yield	Time	% of yield ^{a, b}
1	C ₆ H ₅	45	84 (1a)	50	81 (1a)
2	<i>p</i> -NO ₂ -C ₆ H ₄	45	83 (1b)	50	81 (1b)
3	<i>p</i> -Cl-C ₆ H ₄	50	81 (1c)	55	77 (1c)
4	<i>p</i> -CH ₃ -C ₆ H ₄	50	81 (1d)	60	78 (1d)
5	<i>p</i> -OMe-C ₆ H ₄	55	80 (1e)	60	78 (1e)
6	2-Naphthyl	50	81 (1f)	55	80 (1f)

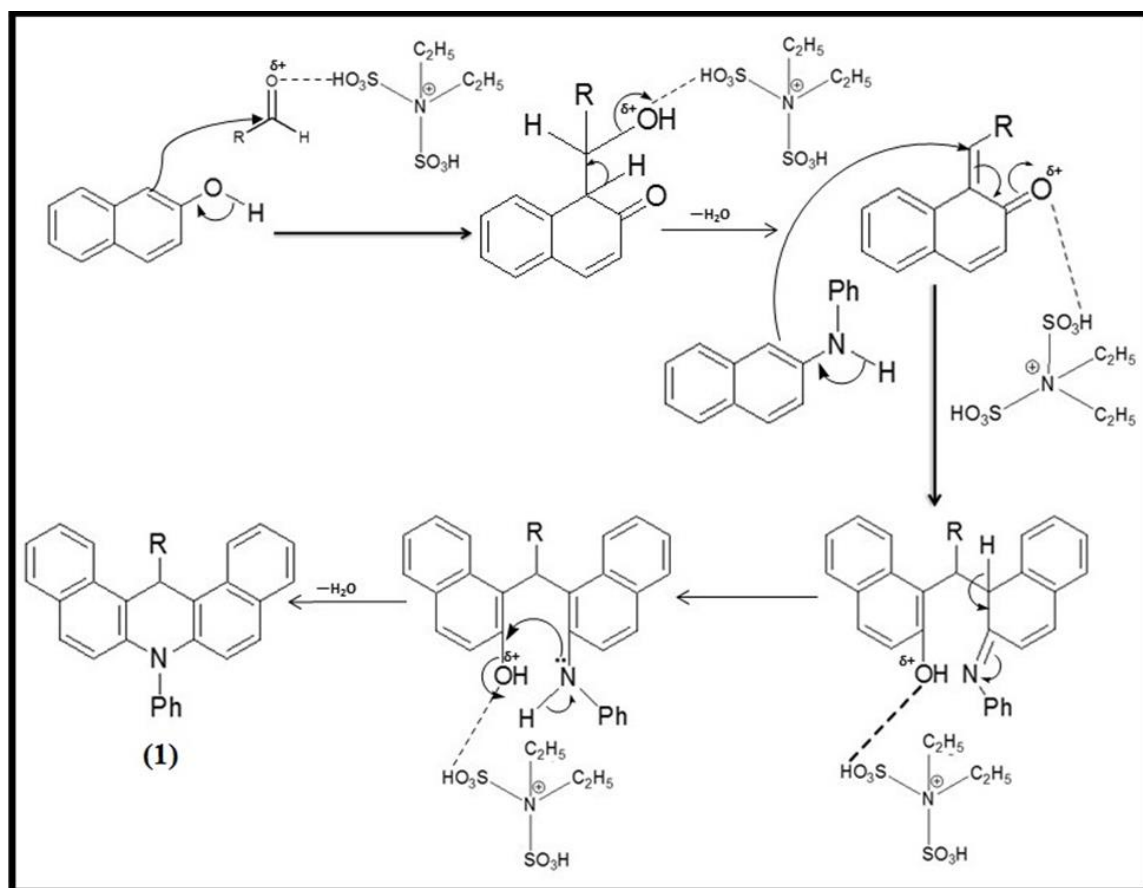
^a Isolated yields ; ^b Reactions were performed at 100 °C under neat condition using **IL-14** and **IL-15**

In order to optimize the reaction condition, the reaction of 2-naphthol, benzaldehyde and N-phenyl-2-naphthylamine was investigated with 15 mol% of [DEDSA][FeCl₄] and [DEDSA]₂[Zn₂Cl₆] salts in three different temperatures (such as 90°C, 100°C and 110 °C) under solvent-free condition for 45-60 min reaction (table-5.3, entries 1-3 and 6-8). Out of these three temperatures, we got the best results at 100 °C as 81-84 % of product (**1a**) were formed within 45-50 min (table-5.3, entries 2, 7) while at 90 °C there was a little drop in reaction rate (table-5.3, entries 3, 8). The model reaction produced aryldi-(2-hydroxy-1-naphthyl)-methane as single product at room temperature in ethanol for 2 hour where we collected N-phenyl-2-naphthylamine as unreacted substrate. The amount of both catalysts was optimized as 10 mol% after investigating the model reaction with 8 mol% and 10 mol% at 100 °C without any solvent (table-5.3, entries 4-5, 9-10).

5.2.2.2. Substrate scope study and plausible mechanism

Thus from the above studies 10 mol% of chlorometallate salt at 100 °C were considered as the optimized condition for generation of complex molecules of dibenzoacridine derivatives through variation of substituted aromatic aldehydes. These results are summarized in the **Table-5.4**. Aromatic aldehyde bearing electron donating or withdrawing group produced very good amount of dibenzoacridine in reasonable reaction time using the two catalysts without any side products (table-5.4, entries 1-6). The overall catalytic activities of [DEDSA]₂[Zn₂Cl₆] and [DEDSA][FeCl₄] salts were observed to be equivalent for the three-component one-pot synthesis of 14-aryl-7-N-phenyl-14*H*-dibenzo[*a,j*]acridine derivatives (**1**) under optimized conditions.

The plausible mechanisms of dibenzoacridine synthesis can be explained via activation of aldehyde through H-bonding with acidic IL followed by nucleophilic attack of 2-naphthol and then subsequent steps according to the reaction **Scheme-5.2**.



Scheme-5.2: Plausible mechanism of synthesis of dibenzoacridine

5.2.2.3. Reusability of catalysts

The reusability study of two heterogeneous catalysts was examined for the model reaction in 5 mmol scale under the optimized conditions in solvent-free medium up to 6th cycles. After each run, the catalyst was recovered from the reaction mixture as solid residue by simple filtration using dichloromethane. Then it was dried in vacuum oven at 80 °C and reused for the next run. These catalysts lost their activities slowly after 3rd cycles as reaction time were increased to produce good amount of dibenzoacridine (**1a**) as shown in **Fig.5.10**. These small changes were also evidenced from the PXRD pattern and ICP-OES analysis of used catalysts included in the **Table-5.2**.

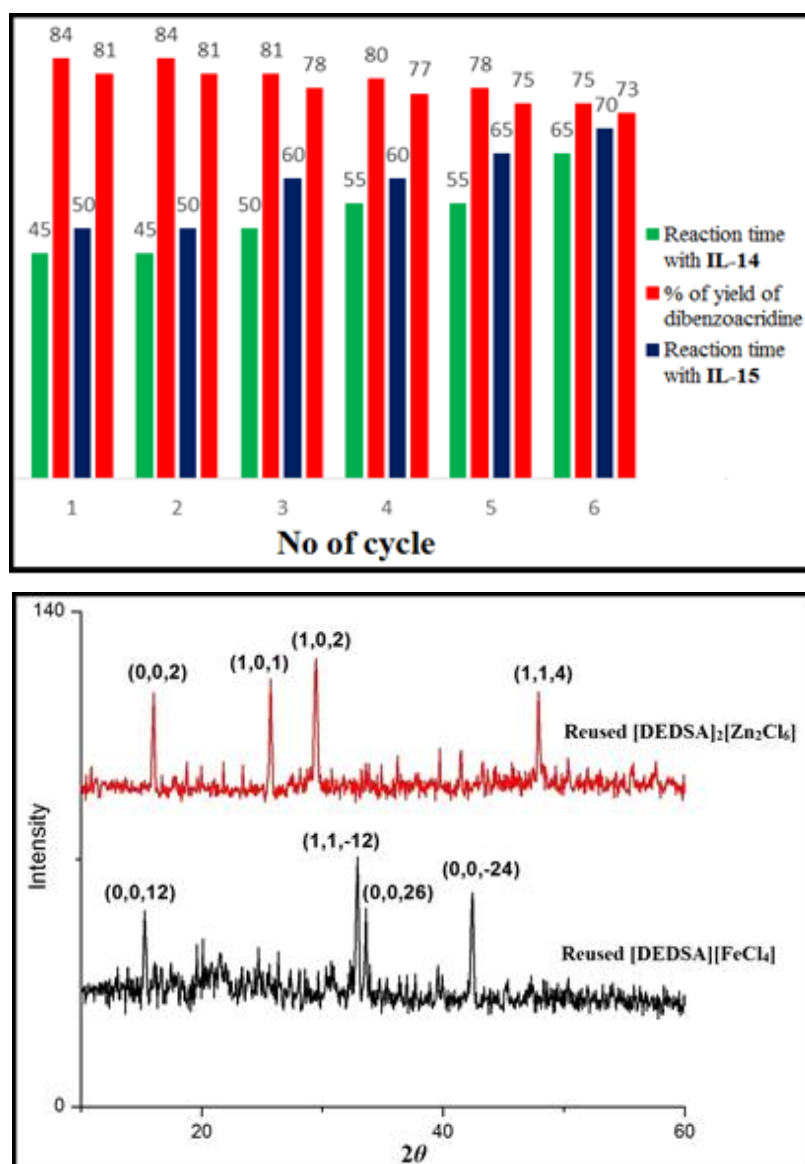


Fig.5.10: (a) Reusability study and (b) Powder XRD characterization after 6th cycle for the spent chlorometallates.

5.2.3. Fluorescence study of 14-aryl-7-(N-phenyl)-14H-dibenzo[a,j]acridine derivatives (1)

The UV-visible absorption spectra of six dibenzoacridine derivatives were taken using 3×10^{-3} M solution of CHCl_3 . All the compounds exhibited single absorption band with absorption maxima (λ_{abs}) around 366-370 nm. Then the same sample solutions were utilized for excitation in the wavelength range of 366-370 nm using a Fluorescence spectrophotometer. The fluorescence emission spectra of the six compounds displayed emission within the range of 380-560 nm corresponding to fluorescence emission maxima around $\lambda_{\text{emi}} = 434$ -440 nm as shown in **Fig.5.11** and **Table-5.5**. The fluorescence quantum yields of the various samples were calculated in the **Table-5.5** using the same equation as already mentioned in the **Chapter-3C** using taking anthracene as standard compound.

The fluorescence intensity was affected due to the presence of different substituent phenyl ring within the acridine derivatives. For example, the acridine derivatives bearing -OMe (**1e**) and -NO₂ (**1b**) group exhibit highest and lowest intensities in the emission spectra respectively.

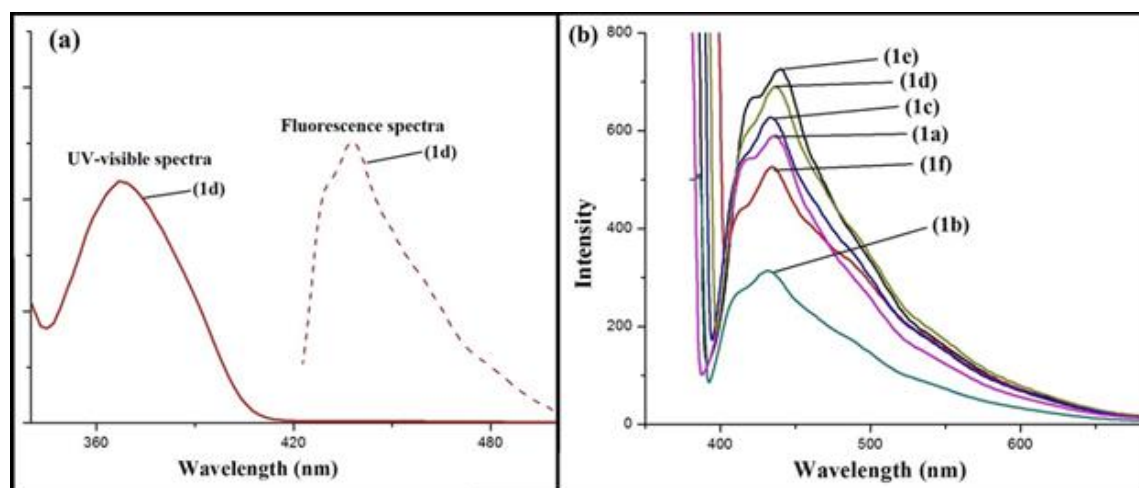


Fig.5.11: UV/Visible absorption and fluorescence emission spectra of benzoacridine derivatives

Table-5.5: Absorption-emission maxima and fluorescence quantum yields of 14-aryl-7-(N-phenyl)-14H-dibenzo[a,j]acridine in chloroform using anthracene as standard.

Entry	Sample	λ_{abs} (nm)	λ_{emi} (nm)	Φ_s
1	1a	366	435	0.21
2	1b	370	434	0.09

3	1c	368	435	0.24
4	1d	366	437	0.28
5	1e	368	440	0.31
6	1f	366	436	0.17

5.3. Conclusion

In summary, we have developed two $-\text{SO}_3\text{H}$ group functionalized diethyl-disulfoammonium chlorometallate ILs, $[\text{DEDSA}]_n[\text{X}]$, where $n = 1$ and 2 for $\text{X} = \text{FeCl}_4^-$ (**IL-14**) and $\text{Zn}_2\text{Cl}_6^{2-}$ (**IL-15**) as solid acidic materials. Their composition and properties were characterized by various spectroscopic and analytical techniques such as NMR, FT-IR, UV/Vis, Raman, PXRD, SEM-EDX, ICP-OES, TGA and CHN analyser. The acidity and thermogravimetric analysis of $[\text{DEDSA}][\text{FeCl}_4]$ and $[\text{DEDSA}]_2[\text{Zn}_2\text{Cl}_6]$ salts also supported their uses as efficient heterogeneous acidic catalysts for the three-component synthesis of 14-aryl-7-(N-phenyl)-14*H*-dibenzo[*a,j*]acridine derivatives for six consecutive cycles under optimized reaction condition. The fluorescence properties were observed for these novel dibenzoacridine derivatives which can open up their further uses in material science.

5.4. Experimental Section

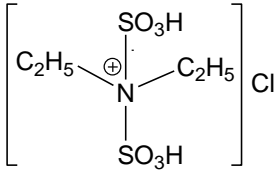
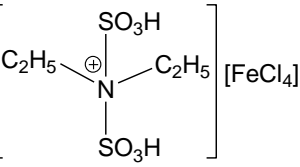
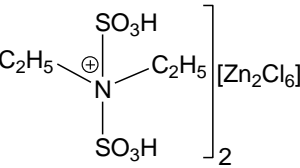
5.4.1. Preparation of diethyl-disulfoammonium chlorometallates $[\text{DEDSA}]_n[\text{X}]$, where $n = 1$ and 2 for $\text{X} = \text{FeCl}_4^-$ (**IL-14**) and $\text{Zn}_2\text{Cl}_6^{2-}$ (**IL-15**)

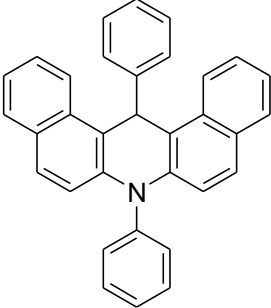
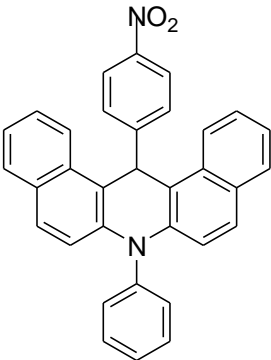
The parent ionic liquid $[\text{DEDSA}][\text{Cl}]$ was prepared by drop wise addition of ClSO_3H (30 mmol) at 0°C to a solution of Et_2NH (15 mmol) in dry CH_2Cl_2 in a two necked 100 mL round bottomed flask fitted with a vacuum system through water and alkali trap for removal of HCl gas. The mixture was stirred continuously at room temperature for another one hour to produce diethyldisulfoammonium chloride $[\text{DEDSA}][\text{Cl}]$ (**IL-13**) as reddish liquid immiscible with CH_2Cl_2 . Then the crude ionic liquid was washed three times with dry CH_2Cl_2 (3 x 5 mL) and dried under vacuum to get analytically pure 98 % of **IL-13**. In next step, the transition metal chlorides were added to the $[\text{DEDSA}][\text{Cl}]$ in their respective mole fractions (0.5 for both FeCl_3 and ZnCl_2) and heated at 80°C for 2 hour under nitrogen atmosphere to get the corresponding chlorometallates $[\text{DEDSA}]_n[\text{X}]$ (**IL-14** to **IL-15**) in solid state with 96-97 % of yield after washing with dry DCM (3 x 10 mL) .

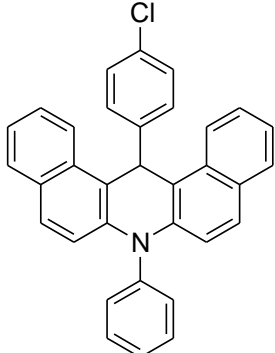
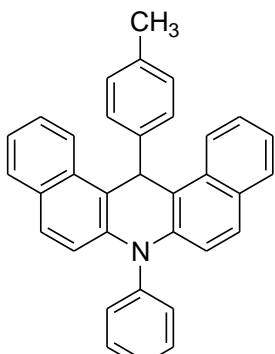
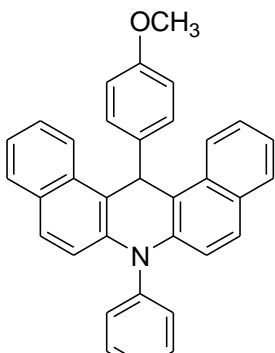
5.4.2. General method for preparation of 14-aryl-7-(N-phenyl)-14H-dibenzo[a,j]acridines derivatives (1)

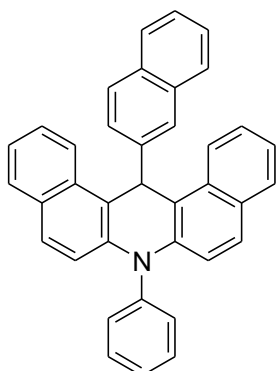
In a 50 mL round bottomed flask, a mixture of 2-naphthol (1 mmol), aldehyde (1 mmol) and N-phenyl-2-naphthyl amine (1 mmol) was heated at 100 °C in presence of 10 mol% of [DEDSA][FeCl₄] or [DEDSA]₂[Zn₂Cl₆] as catalyst under solvent free condition. The course of reaction was monitored by TLC. To the reaction flask, 3 mL of dry dichloromethane was added for dissolving the crude organic product after completion of the reaction. The solution of DCM was filtered for separation of solid residue of catalyst on the filter paper. Then the catalyst was washed with dry DCM (2 x 3 mL) and dried in vacuum oven at 80 °C for the next cycle of the reaction. The dichloromethane solution was dried over anhydrous Na₂SO₄ and then evaporated in rotary evaporator to isolate the crude dibenzoacridine as solid mixture. The crude product was again precipitated from absolute EtOH which provides analytically pure product.

5.4.3. Spectral data of ionic liquids and dibenzoacridine derivatives (1)

Product	Spectral data
	[DEDSA][Cl] (IL-13): Light reddish liquid; FT-IR (KBr): 3410, 1411, 1370, 1147, 1044, 871 cm ⁻¹ ; ¹ H NMR (400MHz, DMSO-d ₆): δ 1.41 (t, 6H, J= 7.32 Hz), 2.82-2.92 (m, 4H), 11.30 (s, 2H) ; ¹³ C NMR (100MHz, DMSO-d ₆): δ 16.7, 54.0; CHN analysis: Calculated for C ₄ H ₁₂ ClNO ₆ S ₂ (%): C 17.81, H 4.48, N 5.19; Found C 17.96, H 4.62, N 5.33.
	[DEDSA][FeCl₄] (IL-14): Light yellow solid; 97% yield; m.p. 117 °C; FT-IR (KBr): 3397, 1427, 1385, 1161, 1049, 869 cm ⁻¹ ; CHN analysis: Calculated for C ₄ H ₁₂ Cl ₄ FeNO ₆ S ₂ (%): C 5.95, H 2.00, N 3.47; Found C 5.91, H 2.06, N 3.52.
	[DEDSA]₂[Zn₂Cl₆] (IL-15): Off white solid; 96% yield; m.p. 122 °C; FT-IR (KBr): 3380, 1408, 1362, 1166, 1052, 879 cm ⁻¹ ; CHN analysis of C ₈ H ₂₄ Cl ₆ Zn ₂ N ₂ O ₁₂ S ₄

	(%): Cal. C 6.36, H 2.13, N 3.71; Found C 6.44, H 2.22, N 3.78.
	<p>14-Phenyl-7-(N-phenyl)-14H-dibenzo[a,j]acridine (1a) (table-5.4, entry 1): Light yellow solid; m.p. 294-296 °C; FT-IR (KBr): 3036, 2970, 1621, 1508, 1409, 1272, 1082, 958, 801, 751 cm⁻¹; ¹H NMR (400MHz, CDCl₃): δ 6.80 (d, 2H, <i>J</i>= 9.2 Hz), 6.94 (s, 1H,), 6.99 (t, 1H, <i>J</i>= 7.3 Hz), 7.13 (t, 2H, <i>J</i>= 7.4 Hz), 7.32 (t, 2H, <i>J</i>= 7.3 Hz), 7.42-7.60 (m, 9H), 7.67-7.77 (m, 4H), 8.50 (d, 2H, <i>J</i>= 8.7 Hz); ¹³C NMR (100MHz, CDCl₃): δ 38.3, 115.7, 116.7, 122.2, 123.3, 126.2, 126.9, 127.5, 127.7, 128.4, 128.7, 129.9, 131.0, 131.6, 131.9, 138.5, 141.2 146.0; CHN analysis: Calculated for C₃₃H₂₃N (%) : C 91.42, H 5.35, N 3.23; Found C 91.34, H 5.42, N 3.28.</p>
	<p>14-(4-Nitrophenyl)-7-(N-phenyl)-14H-dibenzo[a,j]acridine (1b) (table-5.4, entry 2): Light brown solid; m.p. 315-318 °C; FT-IR (KBr): 3029, 2973, 1618, 1501, 1412, 1242, 1071, 966, 811, 737 cm⁻¹; ¹H NMR (400MHz, CDCl₃): δ 6.61 (s, 1H), 6.82 (d, 1H, <i>J</i>= 9.2 Hz), 7.44 (t, 2H, <i>J</i>=8.2 Hz), 7.52 (d, 2H, <i>J</i>= 8.7 Hz), 7.57-7.63 (m, 5H), 7.66-7.76 (m, 4H), 7.83-7.87 (m, 3H), 7.97-8.01 (m, 3H), 8.42 (d, 1H, <i>J</i>= 8.2 Hz), ; ¹³C NMR (100MHz, CDCl₃): δ 37.9, 116.0, 117.0, 118.1, 122.1, 123.8, 123.9, 124.7, 127.3, 129.0, 129.1, 129.7, 131.1, 148.8, 152.1; CHN analysis: Calculated for C₃₃H₂₂N₂O₂ (%) : C 82.83, H 4.63, N 5.85; Found C 82.88, H 4.80, N 5.77.</p>
	<p>14-(4-Chlorophenyl)-7-(N-phenyl)-14H-dibenzo[a,j]acridine (1c) (table-5.4, entry 3): Yellow solid; m.p. 288-289 °C; FT-IR (KBr): 3043, 2954, 1605, 1492, 1394, 1259, 1077, 1010, 948, 807, 757 cm⁻¹; ¹H NMR (400MHz, CDCl₃): δ 6.79 (d, 2H, <i>J</i>= 9.2 Hz), 6.92 (s, 1H,), 7.07-7.10 (m, 3H), 7.31-7.48 (m, 5H), 7.53-7.58</p>

	<p>(m, 4H), 7.69-7.84 (m, 5H), 8.44 (d, 2H, $J = 8.7$ Hz); ^{13}C NMR (100MHz, CDCl_3): δ 37.5, 115.1, 117.0, 118.0, 121.9, 122.5, 123.4, 124.5, 127.0, 127.8, 128.5, 128.8, 128.9, 131.1, 131.5, 138.5, 140.9, 143.5, 144.3, 148.8 ; CHN analysis: Calculated for $\text{C}_{33}\text{H}_{22}\text{ClN}$ (%): C 84.69, H 4.74, N 2.99; Found C 84.77, H 4.84, N 3.03.</p>
	<p>14-(4-Methylphenyl)-7-(N-phenyl)-14H-dibenzo[a,j]acridine (1d) (table-5.4, entry 4): Brown solid; m.p. 306-307 °C; FT-IR (KBr): 3060, 2988, 1614, 1499, 1401, 1266, 1088, 808, 755 cm^{-1}; ^1H NMR (400 MHz, CDCl_3): δ 2.12 (s, 3H), 6.45 (s, 1H), 6.79 (d, 2H, $J = 9.2$ Hz), 6.93 (t, 2H, $J = 8.3$ Hz), 7.32 (t, 2H, $J = 7.3$ Hz), 7.42 (d, 2H, $J = 7.8$ Hz), 7.48 (d, 2H, $J = 8.2$ Hz), 7.51-7.59 (m, 5H), 7.68-7.73 (m, 4H), 8.52 (d, 2H, $J = 8.7$ Hz); ^{13}C NMR (100MHz, CDCl_3): δ 20.9, 37.9, 115.8, 116.7, 122.3, 123.2, 126.8, 127.4, 127.5, 128.6, 129.1, 129.9, 130.9, 131.6, 131.9, 136.0, 138.4, 141.0, 143.2 ; CHN analysis: Calculated for $\text{C}_{34}\text{H}_{25}\text{N}$ (%): C 91.24, H 5.63, N 3.13; Found C 91.30, H 5.66, N 3.18.</p>
	<p>14-(4-Methoxyphenyl)-7-(N-phenyl)-14H-dibenzo[a,j]acridine (1e) (table-5.4, entry 5): White solid; m.p. 274-276 °C; FT-IR (KBr): 3054, 2975, 1606, 1495, 1404, 1251, 1059, 962, 807, 747 cm^{-1}; ^1H NMR (400MHz, CDCl_3): δ 3.61 (s, 3H), 6.79 (d, 2H, $J = 9.2$ Hz), 6.92 (s, 1H), 7.07-7.09 (m, 2H), 7.34-7.45 (m, 6H), 7.53-7.59 (m, 4H), 7.69-7.84 (m, 5H), 8.44 (d, 2H, $J = 8.7$ Hz); ^{13}C NMR (100MHz, CDCl_3): δ 37.5, 115.3, 116.7, 118.2, 121.9, 122.5, 123.5, 124.6, 127.0, 127.8, 128.5, 128.8, 128.9, 130.0, 131.5, 138.5, 141.0, 143.5, 144.3, 148.8; CHN analysis: Calculated for $\text{C}_{34}\text{H}_{25}\text{NO}$ (%): C 88.09, H 5.44, N 3.02; Found C 88.16, H 5.56, N 3.08.</p>



14-Naphthyl-7-(N-phenyl)-14H-dibenzo[a,j]acridine (1f) (table-5.4, entry 6): Yellow solid; m.p. 299-301 °C; FT-IR (KBr): 3039, 2963, 1599, 1492, 1398, 1248, 1066, 960, 804, 741 cm^{-1} ; ^1H NMR (400MHz, CDCl_3): δ 6.66 (s, 1H), 6.83 (d, 2H, $J=9.2$ Hz), 7.29-7.37 (m, 4H), 7.52-7.62 (m, 9H), 7.69-7.74 (m, 6H), 7.93 (s, 1H), 8.61 (d, 2H, $J=8.2$ Hz) ; ^{13}C NMR (100MHz, CDCl_3): δ 38.5, 115.5, 116.8, 122.3, 123.2, 125.7, 126.5, 126.9, 127.4, 127.7, 128.1, 128.4, 128.6, 128.7, 130.0, 131.1, 131.6, 133.2, 138.6, 141.2, 143.2 ; CHN analysis: Calculated for $\text{C}_{37}\text{H}_{25}\text{N}$ (%): C 91.89, H 5.21, N 2.90; Found C 92.01, H 5.28, N 2.85.

References

- [1] Hussey, C.L. *Adv. Molten Salt Chem.* **5**, 185--229, 1983.
- [2] Welton, T. *Chem. Rev.* **99**, 2071--2084, 1999.P.
- [3] Wasserscheid, P., & Keim, W. *Angew. Chem. Int. Ed.* **39**, 3773--3789, 2000.
- [4] Sitze, M.S., et al. *Inorg. Chem.* **40**, 2298--2304, 2001.
- [5] Estager, J., et al. *Inorg. Chem.* **50**, 5258--5271, 2011.
- [6] Estager, J., et al. *Dalton Trans.* **39**, 11375--11382, 2010.
- [7] Estager, J., et al. *Chem. Soc. Rev.* **43**, 847--886, 2014.
- [8] Saikia, S., et al. *J. Mol. Catal. A: Chem.* **416**, 63--72, 2016.
- [9] Gogoi, P., et al. *Appl. Catal. A-Gen.* **492**, 133--139, 2015.
- [10] Dutta, B., et al. *Tetrahedron Lett.* **44**, 8641--8643, 2003.
- [11] Benniston, A.C., & Rewinska, D.B. *Org. Biomol. Chem.* **4**, 3886--3888, 2006.
- [12] Zhang, G., et al. *Synthesis* **2010**, 3993--3998, 2010.
- [13] Osyanin, V.A., et al. *Chem. Heterocycl. Compd.* **50**, 1199--1202, 2014.
- [14] LinLin, W., et al. *Chin. Sci. Bull.* **58**, 3624--3629, 2013.
- [15] Babushkina, O.B., & Volkov, S.V. *J. Mol. Liq.* **83**, 131--140, 1999.
- [16] Devashankar, S., et al. *J. Cryst. Growth* **311**, 4207--4212, 2009.
- [17] Kumar, A., et al. *J. Fundam. Appl. Sci.* **7**, 422--435, 2015.
- [18] Bouma, R.J., et al. *Inorg. Chem.* **23**, 2715--2718, 1984.